Journal of Zhejiang University SCIENCE A
ISSN 1009-3095 (Print); ISSN 1862-1775 (Online)
www.zju.edu.cn/jzus; www.springerlink.com
E-mail: jzus@zju.edu.cn

Simple PSF based method for pupil phase mask's optimization in wavefront coding system

ZHANG Wen-zi, CHEN Yan-ping, ZHAO Ting-yu, YE Zi, YU Fei-hong[†‡]

(*State Key Laboratory of Modern Optical Instrumentation, Optical Engineering Department, Zhejiang University, Hangzhou 310027, China*)

[†]E-mail: feihong@zju.edu.cn

Received Apr. 20, 2006; revision accepted Aug. 21, 2006

Abstract: By applying the wavefront coding technique to an optical system, the depth of focus can be greatly increased. Several complicated methods, such as Fisher Information based method, have already been taken to optimize for the best pupil phase mask in ideal condition. Here one simple point spread function (PSF) based method with only the standard deviation method used to evaluate the PSF stability over the depth of focus is taken to optimize for the best coefficients of pupil phase mask in practical optical systems. Results of imaging simulations for optical systems with and without pupil phase mask are presented, and the sharpness of image is calculated for comparison. The optimized results showed better and much more stable imaging quality over the original system without changing the position of the image plane.

Key words: Wavefront coding, Pupil phase mask, Depth of focus, PSF stability, Optimization, Sharpness, Imaging simulation
doi:10.1631/jzus.2007.A0180 **Document code:** A **CLC number:** O435.2; O438.2; TN202; TN762

INTRODUCTION

Wavefront coding was introduced to increase the depth of focus for optical system in 1995 by Dowski and Cathey (1995). A cubic phase mask was placed in pupil plane to encode the wavefront of the optical system by which the intermediate image formed could almost be invariant in a large depth of focus, and the intermediate image could be digitally restored into clear one. This technique shows wonderful results in extending the depth of focus (Cathey and Dowski, 2002; Gómez-Morales *et al*., 2005; Narayanswamy and Silveira, 2006).

Many approaches have already been taken to explore the best pupil phase mask in ideal conditions. Both spatial and spatial-frequency domains have already been considered, and many types of pupil phase masks have been studied (Abrahamsson *et al*., 2006; Castro and Ojeda-Castañeda, 2005; Chi and Nicholas, 2005; Mezouari and Harvey, 2002; Mezouari *et al*., 2004; Sherif *et al*., 2001). In a previous paper, Prasad *et al*.(2002) introduced the concept of pupil phase engineering (PPE), one Fisher Information based method was applied in spatial domain with full PSF to optimize for the best coefficients of pupil phase mask in ideal condition. However it is a complicated way to use the Fisher Information based metric in practical systems, and it is also difficult to work out the derivatives. Furthermore, only defocus was considered in the Fisher Information based optimization while it is much more complicated for practical optical systems, which may suffer from many aberrations besides defocus.

In this paper we try to optimize for the best coefficients of a symmetric mixed cubic mask used in a cemented doublet system by maximizing the PSF stability over the depth of focus. This type of pupil phase mask shows much more stable PSF over depth of focus, which can be referred to (Prasad *et al*., 2002). As we try to do in a simple way, only the standard deviation (STD) of the full polychromatic PSF over the depth of focus is calculated as the PSF stability,

‡ Corresponding author

and a simple simulated annealing (SA) method is used to search for the best coefficients of pupil phase mask in the coefficients space. Though it is a simple method, the optimized results show good results in extending the depth of focus and it is suitable for any type of pupil phase mask in practical optical systems.

PUPIL PHASE MASK'S OPTIMIZATION BASED ON PSF STABILITY

Though many types of pupil phase mask have been explored, we apply our optimization for the best coefficients of a symmetric mixed cubic phase mask which is of the form $Z=a(X^3+Y^3)+b(X^2Y+XY^2)$ in this section.

Cemented doublet system

An F/5 cemented doublet system with a 100-mm focal length and a ±3° half field of view is chosen as the object system to extend its depth of focus by wavefront coding so that sharp images for objects from 15 m to infinity can be acquired without changing the position of the image plane. A 2D view of this system can be found in Fig.1a. Three wavelengths, which are 656.3 nm, 587.6 nm, and 486.1 nm, are taken into account with equal weight. The polychromatic MTF (modulation transfer function) of this system are plotted in Fig.1b, where the solid, dashed, dotted, and dash-dot lines correspond to the MTF with the object at infinity, 50 m, 30 m, and 15 m, respectively. Within an ideal F/5 lens of 100-mm focal length which is focused at infinity, these object distances correspond to the defocus W_{20}, 0, 1.71, 2.84, 5.67 wavelengths (587.6 nm), respectively. The sagittal and tangential MTF of different field of views (0°, 2°, and 3°) are plotted in lines of the same style. The spot diagram of the system is shown in Fig.1c, below which a scalar bar is shown. Besides defocus, large coma, axial chromatic aberration and astigmatism can be found in Fig.1c. One can conclude that this cemented doublet system cannot work well with object at 30 m, or even 50 m.

For the wavefront encoding system, a glass, BK7_SCHOTT, which is 3 mm thick, is placed 1 mm before the STOP of the original system. The STOP of the new system is set on the first surface of the plate, which will be changed to be of the form $Z=a(X^3+Y^3)+b(X^2Y+XY^2)$ for optimization.

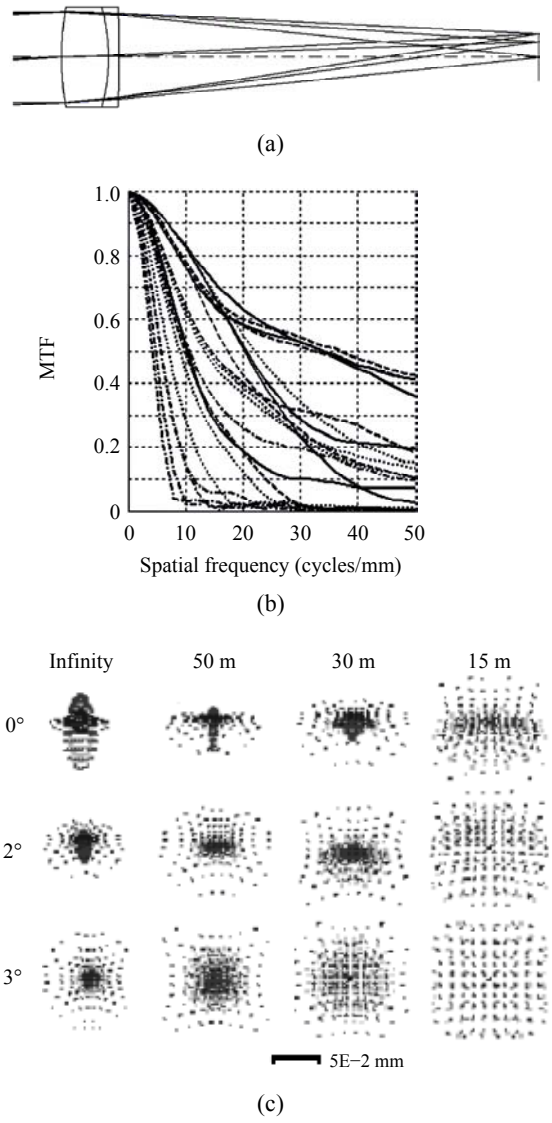

Fig.1 A 2D view (a), MTF (b) and spot diagram (c) of the original cemented doublet system

PSF based optimization

No matter what form the pupil phase mask is, if it can improve the imaging quality of the system by wavefront coding, it should encode the wavefront to form invariant PSF over the depth of focus. So we can try to optimize for the best coefficients of the pupil phase mask by maximizing the PSF stability over the depth of focus. Here the PSF stability over the depth of focus is evaluated by the standard deviation (STD) of the full PSF at all sampled object distances and sampled field positions. The STD value is then divided by the mean PSF value of each grid point for comparison with other grid points in the PSF grid.

Additional penalty for low Strehl ratio is also added, as low Strehl ratio may lead to low MTF, i.e. difficult filtering process. The metric function can be then defined as follows:

$$MF=\frac{\sum_{i}^{X}\sum_{j}^{Y}\frac{STD(\{PSF_{ZF}\}_{i,j})}{Mean(\{PSF_{ZF}\}_{i,j})}}{XY}+\frac{W(1-S.R._{\min})}{\exp(K(S.R._{\min}-S.R._{\text{th}}))+1}, \quad (1)$$

where $STD(\{PSF_{ZF}\}_{i,j})$ and $Mean(\{PSF_{ZF}\}_{i,j})$ stand for the standard deviation value and the mean value of the PSF at (i, j) of the full PSF grid at all sampled object distances and sampled field positions, respectively; X and Y are the numbers of grid points for the full PSF grid in X and Y directions, respectively. The later term in Eq.(1), that is $\frac{W(1-S.R._{\min})}{\exp(K(S.R._{\min}-S.R._{\text{th}}))+1}$, is the additional penalty for low Strehl ratio, where W decides the weight of the penalty, K decides the slope of penalty near the threshold, $S.R._{\text{th}}$ and $S.R._{\min}$ stand for the threshold Strehl ratio and the minimal Strehl ratio of all sampled object distances and field positions, respectively.

Optimization results

Three object distances (object at 50 m, 30 m, and 15 m) and four field positions (0°, 1°, 2°, and 3°) are set and the full polychromatic PSF of 512×512 grid is calculated in the optimization process. The threshold Strehl ratio is chosen to be 0.25%, while W is 3.80 and K is 500. As within the coefficients space, pupil phase mask of symmetric mixed cubic type is symmetric between the 1st and the 3rd quadrants, 2nd and 4th quadrants, no limited bound for b and non-negative bound for a are sufficient. Besides, small bound for b should be set to avoid low MTF. Here the coefficients space used is: $a\in$[0, 1.00E−4], $b\in$[−1.00E−5, 1.00E−5]. A simple simulated annealing (SA) method (Ingber, 1996) with its flow chart shown in Fig.2 is applied to search for the minimal value of the metric function. Though the method may consume a lot of time to search within the coefficients space, it is a simple, global and effective optimization method.

The optimized coefficients are: a=1.33E−5, b=0.00. The effective optical thickness in unit of wavelength (587.6 nm), which provides much information about the wavefront distortion introduced by the mask, is about 12.12 wavelengths. A plot of the unfiltered sagittal and tangential polychromatic MTF of the new system applied with this optimized pupil phase mask is shown in Fig.3. Also a typical unfiltered intermediate PSF is shown in Fig.4a. It is obviously there is no zero point within 50 cycle/mm

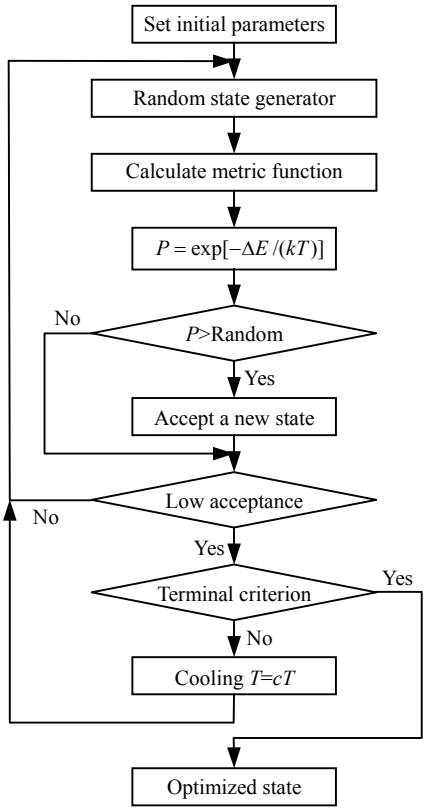

Fig.2 The flow chart of simulated annealing method

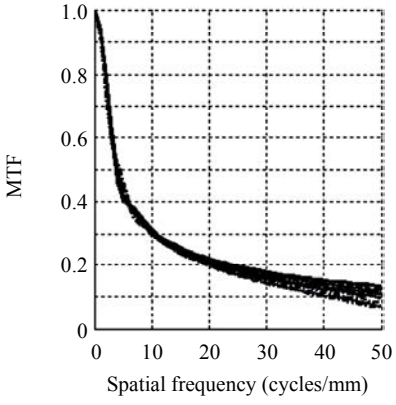

Fig.3 The unfiltered MTF of the system applied with optimized pupil phase mask

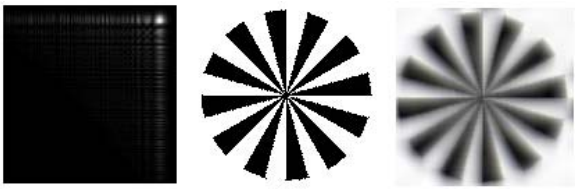

(a) (b) (c)

Fig.4 (a) A typical unfiltered intermediate PSF of the system applied with optimized pupil phase mask; (b) The original object image; (c) The simulated intermediate image corresponding to the PSF of (a)

for sagittal and tangential MTF, even with object at 5 m (not shown in the figure). And they are also much more stable over the depth of focus than the original system.

INTERMEDIATE IMAGE RESTORATION

In this section, we present the imaging simulation results for systems with and without pupil phase mask.

The original image is first decomposed into three channels, i.e. the RGB channels. Each channel's Fourier Spectrum is multiplied by its corresponding wavelength's OTF (optical transfer function), and an inverse Fourier Transform is applied to form the intermediate image. To get the final image, multiply the intermediate Fourier spectrum with the filter spectrum, and take an inverse Fourier Transform. The flow of the imaging simulation process for the wavefront coding system is shown in Fig.5.

The following assumptions are kept in the whole imaging simulation process. (1) No magnification or noise is taken into account; (2) A 128×128 spoke image shown in Fig.4b is used as the original object image; (3) A CCD (charge coupled device) with pixel size of 10 μm is assumed; (4) Only one filter, which is constructed form the mean OTF of object at 50 m, 30 m, and 20 m with their each field positions, is used over the depth of focus for single channel, and the module is limited to be lower than 10.

Simulation result

The simulated images of the original cemented doublet system are shown in Table 1, and the restored images of the system applied with optimized pupil phase mask are shown in Table 2. Only the simulated images with 4 object positions (infinity, 50 m, 30 m, 15 m), and 3 field positions (0°, 2° and 3°) are presented. A typical intermediate image corresponding to the PSF of Fig.4a can be seen in Fig.4c. From Table 1, one can conclude that the original cemented doublet system cannot work well with object at 30 m, or even at 50 m. Much information on the object space is lost in the imaging process. Though there are few brightness fluctuations in the restored images, the wavefront coding system works well within the object at 15 m and sharp image is acquired. The image quality is much more stable, and much more details of the object can be distinguished, i.e. much more in-

Table 1 Simulated images of the original cemented doublet system

Field	Object distance			
	Infinity	50 m	30 m	15 m
0°				
2°				
3°				

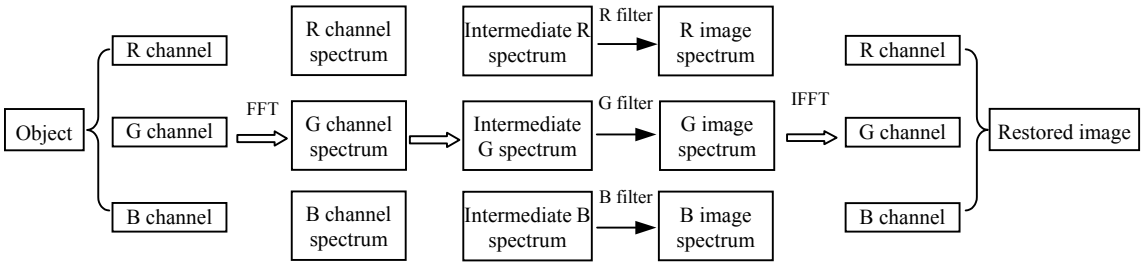

Fig.5 The flow of the imaging simulation process for the wavefront coding system

Table 2 Restored images of the system applied with optimized pupil phase mask

Field	Object distance			
	Infinity	50 m	30 m	15 m
0°	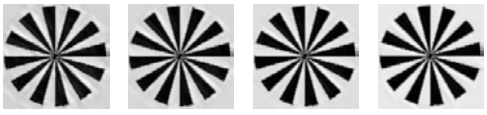			
2°	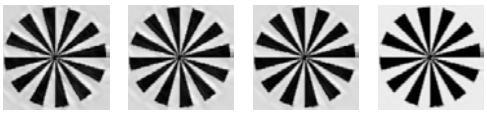			
3°	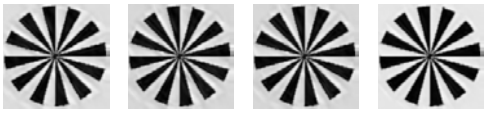			

formation on the object is acquired.

The kernels of the filters for RGB channels are shown in Fig.6a, and the modules of the filters with normalized spatial frequencies are shown in Fig.6b. The average noise gain of the filter is 6.45, which can be calculated as follows:

$$NG=\left[\frac{1}{MN}\sum_{u=0}^{M-1}\sum_{v=0}^{N-1}|F(u,v)|^2\right]^{1/2}, \tag{2}$$

where $F(u,v)$ is the filter in frequency domain with a size of $M\times N$. One may notice that the sagittal and tangential modules are lower than those in diagonal areas. That is the characteristics of pupil phase mask which are of rectangularly separable form. Though the modules of three filters are almost the same, many differences can be found in the kernels. The importance of phase in imaging process should be realized.

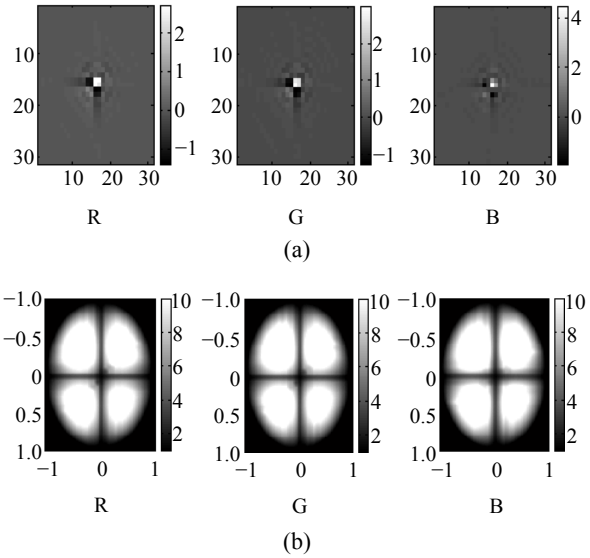

Fig.6 Kernels (a) and modules (b) of RGB filters for the wavefront coding system

Imaging quality evaluation

A simple quantitative method with the sharpness of the image defined according to Energy of Image Gradient function (Subbarao and Choi, 1993) can be taken to evaluate the imaging quality. That is:

$$f(I)=\sum_X\sum_Y\{[I(x+1,y)-I(x,y)]^2+[I(x,y+1)-I(x,y)]^2\}, \tag{3}$$

where I stands for the image to be evaluated, and $I(x,y)$ is the gray value at (x,y) of the image. The ratios of final images' sharpness to sharpness of the original object image are listed in Table 3 and Table 4. It is obvious that the wavefront coding system has advantage in sharpness with respect to the original cemented doublet system, and that it is much more stable over the depth of focus.

Table 3 Sharpness of the images acquired by system without pupil phase mask

Field	Object distance			
	Infinity	50 m	30 m	15 m
0°	0.59074	0.21729	0.12967	0.043440
2°	0.45066	0.38665	0.24396	0.073507
3°	0.23814	0.37416	0.36338	0.147130

Table 4 Sharpness of the images acquired by system applied with optimized pupil phase mask

Field	Object distance			
	Infinity	50 m	30 m	15 m
0°	0.35090	0.36617	0.38213	0.38577
2°	0.34820	0.35934	0.36784	0.40261
3°	0.36006	0.34613	0.34731	0.38841

CONCLUSION

It is convenient to apply this simple PSF based method to optical systems with only the standard deviation method used to evaluate the PSF stability over the depth of focus, both the calculation of the

metric function and the implantation of SA method are easy jobs, and no calculation of derives is involved in the whole optimization process. Still good imaging quality is acquired and the depth of focus is extended. However further research need to be carried out. The cubic phase mask has disadvantages in its rectangularly separable characteristics, with which low sagittal or tangential MTF may lead to lower diagonal MTF, i.e. more difficult filtering process. Higher sagittal and tangential MTF will be needed for further improvement of the system.

References

Abrahamsson, S., Usawa, S., Gustafsson, M., 2006. A new approach to extend focus for high-speed, high-resolution biological microscopy. *Proc. SPIE*, **6090**:60900N-1-60900N-8. [doi:10.1117/12.647022]

Castro, A., Ojeda-Castañeda, J., 2005. Increased depth of field with phase only filters: ambiguity function. *Proc. SPIE*, **5827**:1-11. [doi:10.1117/12.605282]

Cathey, W.T., Dowski, E.R., 2002. New paradigm for imaging systems. *Appl. Opt.*, **41**:6080-6092.

Chi, W.L., Nicholas, G., 2005. Smart camera with extended depth of field. *Proc. SPIE*, **6024**:602424-1-602424-6. [doi:10.1117/12.666949]

Dowski, E.R., Cathey, W.T., 1995. Extending depth of field through wavefront coding. *Appl. Opt.*, **34**:1859-1866.

Gómez-Morales, F., Tudela, R., Ferré-Borrull, J., Bosch, S., de la Fuente, M., 2005. Pupil filters for wavefront coding: off axis performances. *Proc. SPIE*, **592637**:592637-1-592637-7.

Ingber, L., 1996. Adaptive simulated annealing (ASA): Lessons learned. *J. Control and Cybernetics*, **25**(1):33-54.

Mezouari, S., Harvey, A.R., 2002. Primary aberrations alleviated with phase pupil filters. *Proc. SPIE*, **4768**:21-31. [doi:10.1117/12.482192]

Mezouari, S., Muyo, G., Harvey, A.R., 2004. Amplitude and phase filters for mitigation of defocus and third-order aberrations. *Proc. SPIE*, **5249**:238-248. [doi:10.1117/12.516542]

Narayanswamy, R., Silveira, P.E.X., 2006. Iris recognition at a distance with expanded imaging volume. *Proc. SPIE*, **6202**:62020G-1-62020G-12. [doi:10.1117/12.666883]

Prasad, S., Torgersen, T.C., Pauca, V.P., Plemmons, R.J., van der Gracht, J., 2002. Engineering the Pupil Phase to Improve Image Quality. Proc. 2002 AMOS Technical Conference, Maui, HI.

Sherif, S.S., Dowski, E.R., Cathey, W.T., 2001. A logarithmic phase filter to extend the depth of focus of incoherent hybrid imaging systems. *Proc. SPIE*, **4471**:272-279. [doi:10.1117/12.449345]

Subbarao, M., Choi, T., 1993. Focusing techniques. *J. Opt. Eng.*, **32**(11):2834-2836.